Fungal Anthraquinone Photoantimicrobials Challenge the Dogma of Cationic Photosensitizers

Fabian Hammerle[1,#], Johannes Fiala[1,2#], Anja Höck[1], Lesley Huymann[1,2], Pamela Vrabl[2], Yurii Husiev[3], Sylvestre Bonnet[3], Ursula Peintner[2], and Bianka Siewert[1]*

[1] Department of Pharmacognosy, Institute of Pharmacy, University of Innsbruck, Innsbruck, Austria

[2] Institute of Microbiology, University of Innsbruck, Innsbruck, Austria

[3]Leiden Institute of Chemistry, Leiden University, Einsteinweg 55, 2333CC Leiden, The Netherlands

# These authors contributed equally.

* Corresponding author Bianka.siewert@uibk.ac.at

1. Abstract

The photoantimicrobial potential of four mushroom species (i.e., *Cortinarius cinnabarinus, C. sanguineus*, *C. rubrophyllus*, and *C. holoxanthus*) was explored based on a light modified EUCAST protocol. The extracts were tested against *Candida albicans*, *Escherichia coli*, and *Staphylococcus aureus* under blue (λ = 428 nm and λ = 478 nm, H = 30 J cm^{-2}) and green light (λ = 528 nm, H = 30 J cm^{-2}) irradiation. Three extracts showed significant photoantimicrobial effects at concentrations below 25 µg/mL. Targeted isolation of the major pigments from *C. sanguineus* led to the identification of two new potent photoantimicrobials, one of them (i.e., dermocybin) being active against *S. aureus* and *C. albicans* under green light irradiation ($PhotoMIC^{523}$ = 39.5 µM and 2.3 µM, respectively) and the other one (i.e., emodin) being active against *E. coli* in a low micromolar range ($PhotoMIC^{428}$ = 11.1 µM). Intriguingly, dermocybin was not (photo)cytotoxic against three tested cell lines adding an additional level of selectivity. Since both photoantimicrobials are not charged, this discovery shifts the paradigm of cationic photosensitizers.

2. Keywords

Fungal photosensitizers, photoantimicrobials, aPDT, PDI, PACT, dermocyboid *Cortinarii*, emodin, dermocybin, *Cortinarius sanguineus*, *Escherichia coli, Candida albicans, Staphylococcus aureus*

3. Highlights

- Fungal anthraquinones are potent photoantimicrobials
- Dermocybin is a selective photoantimicrobial agent which is not photocytotoxic
- Emodin, a neutral photosensitizer, is characterized by a PhotoMIC of 11 µM against the gram-negative bacterium *E. coli*
- Emodin shows a PhotoMIC of 0.37 µM against *Candida albicans*

4. Introduction

Microbial resistances are inescapable and omnipresent not only in hospitals but also in centuries-old mummies, permafrost, and remote reaches of the ocean (Fisher and Mobashery, 2016). Still, according to the World Health Organization (WHO, 2021), antimicrobial resistance is one of today's greatest global threats. Next to antimicrobial stewardship, developing new treatment strategies and antimicrobials is imperative to limit the dystopic predictions of 10 million deaths per year in 2050 (O'Neill, 2016). In 2017, a list was published by the WHO, categorizing twelve microorganisms into

three R&D priority classes (i.e., critical, high, and medium) for new antibiotics next to *Mycobacterium tuberculosis* (WHO, 2017). In this list, five of the six nosocomial ESKAPE organisms (Rice, 2008) are included (i.e., *Enterococcus faecium, Staphylococcus aureus*, *Acinetobacter baumannii*, *Pseudomonas aeruginosa*, and *Enterobacter spp.*). According to the committee establishing this catalog, future development should generally focus on antimicrobials active against tuberculosis and gram-negative bacteria (Tacconelli et al., 2018).

A special type of antimicrobials, called photoantimicrobials, belongs to one of the emerging treatment strategies for microbial infections, i.e., the antimicrobial photodynamic therapy (aPDT), which is also called photoantimicrobial chemotherapy (PACT) or photodynamic inhibition (PDI) (Wainwright et al., 2017; Wegener et al., 2017; Wainwright, 2019; 2020; Ran et al., 2021). The combination of light and a drug induces lethal signals in microorganisms where well-established antimicrobials fail. Intriguingly, resistances to photoantimicrobials have not yet been observed in the treated microorganisms (Wainwright et al., 2017). Thus, PACT is especially promising for treating local infections caused by multidrug-resistant microbes (Wainwright et al., 2017; Wainwright, 2020; Galstyan, 2021). For example, chlorin e6 –a natural photosensitizer isolated from the alga chlorella (*Chlorella ellipsoidea*)– is photoactive against fifteen isolated drug-resistant strains of *S. aureus* (Aroso et al., 2019).

Crucial parameters for such photosensitizers are the photoyield (i.e., the percentage of absorbed light which is transformed into the toxic reactive oxygen species singlet oxygen) and the absorbance spectra (Lan et al., 2019). In particular, for photoantimicrobials cellular uptake is essential (Galstyan and Dobrindt, 2018; Klausen et al., 2020), especially for gram-negative bacteria, such as *Escherichia coli* (Sperandio et al., 2013). The partial negative character of their outer membrane impedes the uptake of neutral or negatively charged photosensitizers (Wainwright, 2018; Pang et al., 2020). Thus, gram-negative bacteria are relatively resistant to aPDT (or PACT) compared to gram-positive bacteria, which take up photosensitizers more easily due to their porous peptidoglycan layers. Consequently, an established dogma of the PACT says cationic photosensitizers are needed to effectively treat gram-negative bacteria (Sperandio et al., 2013; Ran et al., 2021). One hypothesized mode of action is that cationic photosensitizers will more likely interact with the membrane and thus, enable its lethal disruption by light irradiation. As consequence of this accepted principle, most of the new photosensitizers against gram-negative bacteria are characterized by at least one positive charge (Maisch et al., 2014; Wainwright et al., 2015; Bresolí-Obach et al., 2018).

As part of our ongoing efforts to investigate photosensitizers from mushrooms (i.e., from fruiting bodies of basidiomycetes) (Siewert, 2021), we were interested in exploring the potential of the colorful *Dermocybe* group against different microorganisms. Dermocybes are known for their brightly colored gills, which is due to their versatile (pre)-anthraquinones and were until recently recognized as a subgenus of the species-rich genus *Cortinarius* belonging to the family *Cortinariaceae*. However, recent findings suggest that the family can be subdivided into ten individual genera (Liimatainen et al., 2022). They are characterized by a non-hygrophanous pileus and a non-bulbous stem next to their cortina or the residue of it on the stem. In 2010, Beattie et al. screened 117 collections of Australian *Dermocybes* against *S. aureus* and *Pseudomonas aeruginosa,* finding promising activities based on polyketides (Beattie et al., 2010). Recently, we could show that promising photosensitizers are produced by representatives of related species (Hammerle et al., 2022b). *Cortinarius uliginosus,* as an example, produces the dimeric anthraquinone 7,7'-biphyscion, which was active in the nanomolar range under blue light irradiation against cells of several cancer cell lines (Hammerle et al., 2022a). However, the photoantimicrobial potential of the dermocybes' pigments was, despite one-single observation (Siewert et al., 2022), not studied in detail. Here, we report on the photoantimicrobial screening of *Cortinarius cinnabarinus, C. sanguineus*, *C. malicorius*, and *C. holoxanthus*, as well as the isolation and characterization of the photoantimicrobials from *C. sanguineus*.

5. Results and Discussion

5.1. Initial Photoantimicrobial Screening of *Dermocyboid Cortinarii*

Extracts of the four dermocyboid *Cortinarii* (Table S1) were prepared with acidified acetone. After evaporating the solvent, the dried extracts were dissolved in DMSO and submitted to a primary photoantimicrobial screening, consisting of (i) a HPLC-DAD-MS profiling to characterize the pigmentation profile, (ii) the DMA-assay to test the extracts' ability to produce singlet oxygen in a cell-free environment (Figure S1), and (iii) a photoantimicrobial assay to explore any relevant photoactivity. As depicted in Figure S2, the pigment profile across the fruiting bodies of the four selected fungi varied intensely for all but *C. rubrophyllus* and *C. sanguineus*, which are more closely related. The main pigments (at a detection wavelength of λ = 468 nm, Figure S2) were annotated by comparing the UV/Vis and MS traces with in-house data (refer to Supplementary Part Figure S3 and S4). In detail, cinnalutein was annotated as the main orange pigment in *Cortinarius cinnabarinus*, flavomannin-6,6'-dimethyl ether (FDM) for *C. holoxanthus*, and emodin for *C. rubrophyllus* and *C. sanguineus.* These observations are in agreement with the literature (Gill and Steglich, 1987) and our previous insights (Hammerle et al., 2022b). In the next step, the extracts were submitted to the DMA assay, determining the relative singlet oxygen production as compared to berberine. The assay (Figure S1) revealed that under blue light irradiation, *C. cinnabarinus* is the most efficient producer of singlet oxygen ($\eta_{\Delta, BL}$ = 201%), followed by *C. sanguineus* ($\eta_{\Delta, BL}$ = 151%), *C. rubrophyllus* ($\eta_{\Delta, BL}$ = 144%), and *C. holoxanthus* ($\eta_{\Delta, BL}$ = 64%).

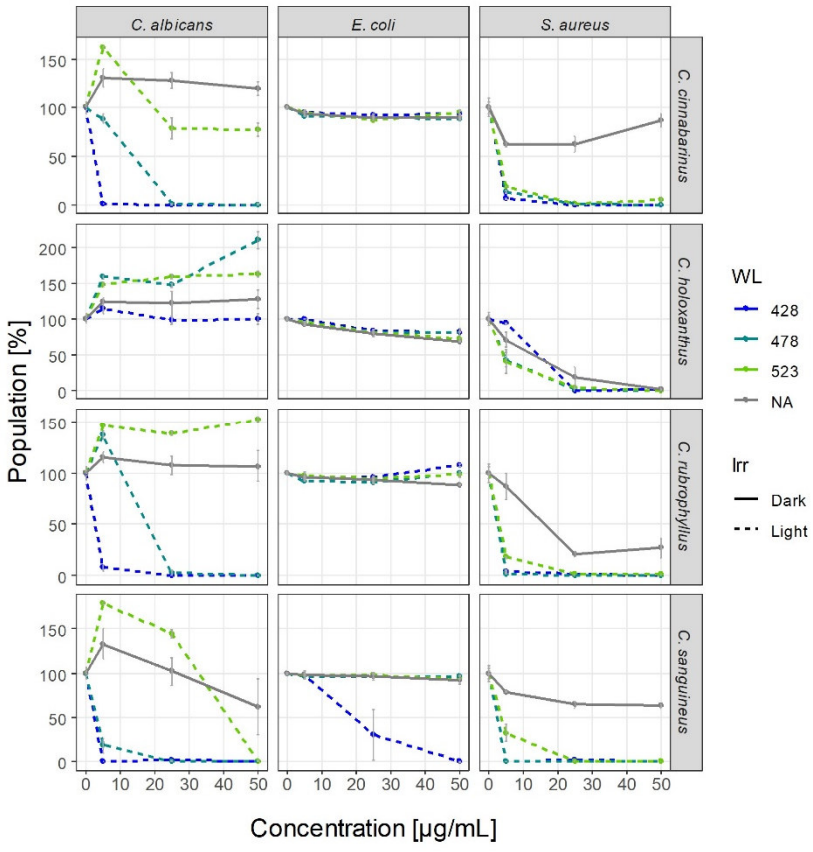

Figure 1. Dose-response curves of the extracts against the three tested microorganisms under irradiation (dotted lines, violet, blue, and green, all 30 J/cm²) as well as in the dark. WL = Wavelength, Irr = Irradiation condition.

A similar trend was observed under green light irradiation, though the difference between the yellow *C. holoxanthus* ($\eta_{\Delta, GL}$ = 33%) and the orange *C. rubrophyllus* ($\eta_{\Delta, GL}$ = 48%) as well as *C. sanguineus* ($\eta_{\Delta, GL}$ = 58%) decreased. The latter can be reasoned by the lack of pigments absorbing green light as observed in the HPLC-DAD chromatogram detected at λ = 519 nm (Figure S3).

The antimicrobial screening (Figure 1) of the extracts revealed great variability across the four different species: While all extracts produced singlet oxygen, the antibacterial activity of the *C. holoxanthus* extract against *S. aureus* was independent from the irradiation parameters (i.e., blue light, green light, or darkness) and determined to be between c = 25 and 50 µg/mL. Thus, *C. holoxanthus* seems to contain at least one classic antimicrobial. One main component of the *C. holoxanthus* extract is flavomannin-6.6'-dimethyl ether (FDM). Studies exploring its antimicrobial effect are nonexistent, though the related fungal metabolite flavomannin A was studied in detail. In 2013, it was shown that the different atropisomers of flavomannin A hold a MIC of approx. 16 µg/mL (c = 29.3 µM) against *S. aureus* (ATCC 29213) (Bara et al., 2013). Thus, the antimicrobial activity might be explained by FDM. The other three extracts could be characterized by a wavelength-dependent photoantimicrobial effect against *C. albicans* and *S. aureus*. With PhotoMICs below or around c = 5 µg/mL, the extracts of *C. cinnabarinus*, *C. rubrophyllus*, and *C. sanguineus* were highly active. This is –besides an initial observation regarding *C. rubrophyllus,* which was reported previously by us (Siewert et al., 2022)– the first systematic proof of the photoantimicrobial potential of these mushrooms.

Of particular interest, however, was the observed activity of *C. sanguineus* against the gram-negative bacterium *E. coli*. An activity against gram-negative bacteria is of importance as four of the six ESKAPE organisms are gram-negative bacteria (i.e., *Klebsiella pneumoniae*, *Acinetobacter baumannii*, *Pseudomonas aeruginosa*, and *Enterobacter spp.*) and thus, treating gram-negative bacteria is one of the most critical therapeutic challenges today (Mulani et al., 2019; Oliveira et al., 2020). The fact that the known pigments of these fruiting bodies are all uncharged, but instead neutral aromatic compounds, challenges the dogma that a positive charge is essential for PS to show any photoactivity against gram-negative bacteria. To identify the active principle, the red extract of *C. sanguineus* was submitted to photoactivity-guided isolation.

5.2. Targeted Isolation of Anthraquinones from *Cortinarius sanguineus*

Extracts of different polarities (i.e., petroleum ether (PE), dichloromethane (DCM), and methanol (MeOH)) were prepared first to narrow down the chemical nature of the photoantimicrobial principle of the bloodred webcap (*C. sanguineus*). Evaporation of the extraction solvents yielded extracts in the form of highly viscous solids, which were redissolved in DMSO and subjected to a HPLC-DAD analysis as well as to the photoantimicrobial testing. The liquid-chromatographic analysis at λ = 468 nm (Figure S6) revealed that the DCM extract quantitatively contained the most anthraquinones. However, the variability of enriched anthraquinones was more limited in the DCM extract compared to the methanol extract. While the methanol extract consisted of monomeric and glycosylated anthraquinones, only the monomeric anthraquinones emodin (**4**) and dermocybin (**5**) were annotated in the DCM extract (Table S2).

The photoantimicrobial assay (Figure S5) showed that the photoactivity against *C. albicans* and *S. aureus* was retained, though the dark toxicity increased at least for the apolar DCM extract. Nevertheless, the PhotoMIC values of all fractions were determined to be between c = 2 and 3 µg/mL, which demonstrates the photoantimicrobial potential of this fungal species. Against *E. coli*, the DCM extract showed a promising PhotoMIC of 3 µg/mL after irradiation at λ = 428 nm. By comparing the chromatograms of the extracts detected at λ = 428 nm and λ = 468 nm, emodin was identified as

putative active principle, as the other compounds were less concentrated in the extract. However, for the activity against *S. aureus* and *C. albicans*, a clear hypothesis could not be drawn as all three fractions showed activity. Thus, the two main components of the DCM extract and the glycosylated compounds of the polar region were isolated by different techniques (i.e., column chromatography, liquid-liquid extraction, and recrystallization) to test the photoantimicrobial potential of the individual compounds. In summary, five anthraquinones previously described (Steglich et al., 1969; Steglich and Lösel, 1972) were isolated from *C. sanguineus* (Figure 2). One of them, dermocybin-1-*O*-β-D-glucopyranoside (**3**), was – for the first time chemically – characterized by means of UV/Vis-spectroscopy (Figure S9), IR-spectroscopy (Figure S7), MS-spectrometry, and NMR-spectroscopy (Figure S12-14). In Table S2 the compiled NMR characterization of **3** and **5** is given.

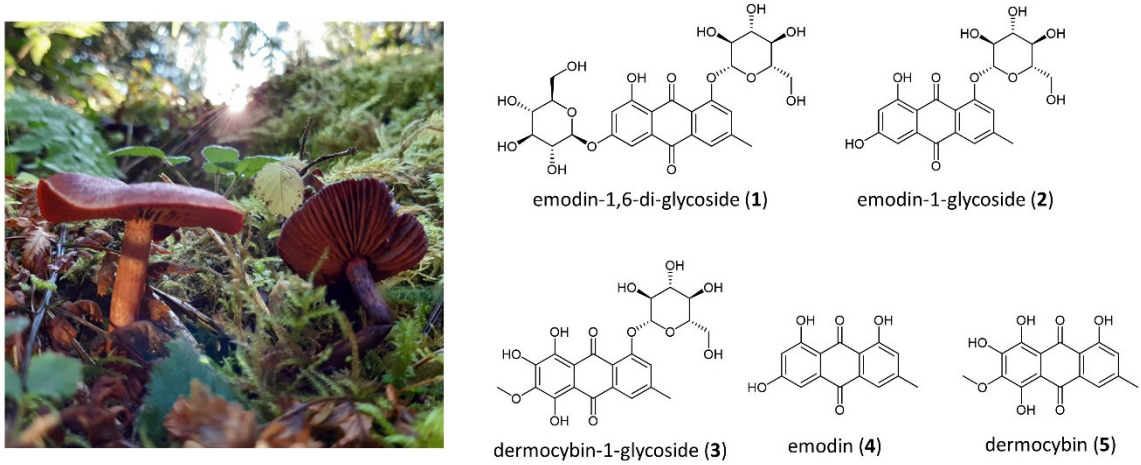

Figure 2 Left) Photograph of two C. sanguineus fruiting bodies; Right) isolated anthraquinones from C. sanguineus.

5.3. Photochemical and Photobiological Evaluation of Emodin (4) and Dermocybin (5)

The isolated monomeric anthraquinones of the most active fraction (DCM) and the glycosylated anthraquinones of the methanolic fraction, being active against *S. aureus*, were photophysically examined. As listed in Table 1, emodin (**4**) was -in terms of the singlet oxygen photoyield- the most active anthraquinone of *C. sanguineus*, correlating with our insights from *C. rubrophyllus* (Hammerle et al., 2022b). In contrast, the bright pinkish dermocybin (**5**), holding two additional hydroxyl groups at positions 5 and 7, was a poor PS. The two additional hydroxyl groups induced a bathochromic shift of nearly $\Delta\lambda$ = 100 nm. Glycosylation of one hydroxyl group and thus the modification of the inductive effect did not affect the VIS absorbance pattern nor the singlet oxygen yield but decreased the molar extinction coefficient ε. In analogy, emodin (**4**) and its monoglycosylated derivative (**2**) were characterized by a similar absorbance pattern and a decrease in the absorbance coefficient. The singlet oxygen photoyield decreased by a factor of approximately two due to the glycosylation. Intriguingly, for **1**, a second glycoside induced an observable hypochromic effect and a drastic epsilon reduction, but no further decrease of the singlet oxygen quantum yield.

Table 1. Photophysical characteristics of the anthraquinone metabolites isolated from C. sanguineus.

Compound	λ_{max} (ε) MeOH [nm (l mol^{-1} cm^{-1})]	λ_{max} (ε) ACN [nm (l mol^{-1} cm^{-1})]	ϕ_Δ (MeOD)	ϕ_Δ (ACN)
1	221 (4398), 264 (3551), 414 (1328)	220 (1680), 264 (1256), 282sh (1021), 411 (461)	0.09	0.02
2	212 (25970), 252 (19466), 287 (17096), 428 (6239)	216 (24888), 252 (17305), 267 (16990), 284 (19004), 416 (7313)	0.11*	0.02
3	215 (33720), 264 (29257), 485 (10742), 525sh (6869)	214 (28233), 264 (24783), 437 (8885), 363 (4960), 522sh (5085)	0.01	0.01
4	226 (16806), 287 (17167), 436 (10724)	222 (36083), 254 (16819), 266 (18235), 288 (19063), 433 (11755)	0.28*	0.49
5	219 (31518), 262 (28581), 277 (23518), 459sh (12966), 484 (15450), 517 (11202)	218 (22927), 261 (22106), 275sh (17836), 303 (8052), 459sh (9911), 483 (12099), 514sh (8106)	0.04	0.01

Perinaphthenone is used as a reference with reported Φ_Δ ($^1O_2$) = 0.98 ± 0.07 in air-saturated ACN (Oliveros et al., 1991). $Ru(bpy_3)Cl_2$ is used as validation compound with reported Φ_Δ ($^1O_2$) = 0.57 ± 0.06 in air-saturated ACN (Garcìa-Fresnadillo et al., 1996). All the samples were dissolved in V = 3 mL of ACN or MeOD and transferred into a macro fluorescence cuvette (Firefly; light path: 1 cm x 1 cm). The $^1O_2$ phosphorescence was measured at 298 K using 450 nm fiber-coupled laser set to 80 mW. The NIR emission spectrums were acquired within 20 s. *Values adapted from (Hammerle et al., 2022b)

As glycosylation is accepted as energy storage principle in Nature, the enrichment of glycosylated anthraquinones in the fruiting bodies might have resulted from this triadic benefit: (i) The photosensitizer is deactivated as compared to the aglycon and thus less harmful for the fungi itself, (ii) it is a convenient energy storage and the water solubility is enhanced, combined with (iii) a sophisticated defense function being activated via the metabolism of the fungivore. Next, the PhotoMICs of the isolated compounds were determined according to a modified EUCAST protocol (Fiala et al., 2021). The MIC itself is defined as the lowest concentration at which the absence of microbial growth can be detected. For each compound, a series of at least ten different concentrations was tested in biological triplicates against *C. albicans*, *E. coli*, and *S. aureus*. As negative control of the light-dependent effect served an identical plate kept in the dark. Table 2 summarizes the obtained results. While all glycosides were inactive, the monomeric anthraquinones dermocybin (**5**) and emodin (**4**) were of particular interest.

Table 2 PhotoMIC values and MIC values of the isolated anthraquinones from Cortinarius sanguineus. Preincubation time was set to t = 60 min.

PS	Irradiation	***Candida albicans***	***Escherichia coli***	***Staphylococcus aureus***
1	428 nm (30 J/cm²)	>84 µM 50.00 mg/L	>84 µM 50.00 mg/L	>84 µM 50.00 mg/L
	478 nm (30 J/cm²)			
	523 nm (30 J/cm²)			
	Dark			
2	428 nm (30 J/cm²)	>115 µM 50.00 mg/L	>115 µM 50.00 mg/L	>115 µM 50.00 mg/L
	478 nm (30 J/cm²)			
	523 nm (30 J/cm²)			
	dark			
3	428 nm (30 J/cm²)	>105 µM 50.00 mg/L	>105 µM 50.00 mg/L	>105 µM 50.00 mg/L
	478 nm (30 J/cm²)			
	523 nm (30 J/cm²)			
	dark			
4	428 nm (30 J/cm²)	0.37 µM 0.10 mg/L	11.1 µM 3.00 mg/L	1.85 µM 0.50 mg/L
	478 nm (30 J/cm²)	2.78 µM 0.75 mg/L	>92 µM 25.00 mg/L	1.85 µM 0.50 mg/L
	523 nm (30 J/cm²)	46 µM 12.50 mg/L	>92 µM 25.00 mg/L	11.1 µM 3.00 mg/L
	dark	>92 µM 25.00 mg/L	>92 µM 25.00 mg/L	>92 µM 25.00 mg/L
5	428 nm (30 J/cm²)	39.5 µM 12.50 mg/L	>79 µM 25.00 mg/L	39.5 µM 12.50 mg/L
	478 nm (30 J/cm²)	19.7 µM 6.25 mg/L		4.74 µM 1.50 mg/L
	523 nm (30 J/cm²)	39.5 µM 12.50 mg/L		2.37 µM 0.75 mg/L
	dark	>79 µM 25.00 mg/L		>79 µM 25.00 mg/L

Dermocybin (**5**) was the most active compound under green light irradiation. A concentration as low as c = 2.37 µM or 0.75 µg/mL was enough to impede growth of the gram-positive bacteria *S. aureus*. While **5** showed only a limited ability to transform the absorbed photoenergy into singlet oxygen, it can be assumed that it rather acts as a PDT type 1 than type 2 photosensitizer. The possibility to induce the photo-effect by green-light irradiation is of special interest due to the deeper penetration depth compared to blue one. Furthermore, an *in vitro* cytotoxicity assay employing mammal cell lines (Table 3) revealed that **5** is only moderately toxic; weak toxicity (EC_{50} = 16.2 µM) was observed under green light irradiation against cells of the lung cancer cell line A549, while it was non-toxic in the dark. **5** was not cytotoxic against the stomach cell line AGS, neither in the dark nor under irradiation. Nevertheless, the light-induced effect, in general, is not as strong as the one of emodin (**4**), which can be rationalized by the low singlet oxygen photoyield. Dermocybin (**5**) might act as a mixed type PS (i.e., PDT type I and type II), however, further studies are needed to explore its mode-of-action in detail.

In contrast to dermocybin (**5**), **4** is active against all three microorganisms tested. *C. albicans* and *S. aureus* were killed by **4** at a dose as low as c = 0.37 µM and 1.85 µM, respectively, when irradiated close to its absorbance maximum. Therewith, emodin (**4**) is even more active as a derivative (i.e., 3-(Bis(3-(dimethylamino)propyl)amino)-7-(di-n-propylamino)phenothiazinium iodide) of the established photosensitizer methylene blue, which is characterized by a PhotoMIC of 3.13 µM against *C. albicans* (Wainwright et al., 2015). Also, compared to the related natural product aloe-emodin (log6 reduction achieved with c = 10 µM, t_{PI} = 30 min, λ = 400-780 nm, H = 24.8 J cm^{-2}, (Ma et al., 2021)) **4** seems to be more promising. Most strikingly, **4** was active against the gram-negative bacterium *E. coli*, contrasting the current state of knowledge (i.e., the requirement of a cationic character for a photosensitizer to be active against gram-negative bacteria (Sperandio et al., 2013; Ran et al., 2021). It seems that the neutral and flat anthraquinone with a logP of 3.641 can penetrate the outer membrane and is thus able to kill the bacterium when light-triggered. Though its photophysical properties and especially its ability to produce singlet oxygen have been known since 1992 (Gollnick et al., 1992), the exploration of its photoantimicrobial effect was done for the first time. Furthermore, **4**'s high activity is of special interest: for other photoantimicrobials like for example for the related hypericin, an optimal concentration against *E. coli* of c = 36 µM (t_{PI} = 68 min, λ = 590 nm, H = 5.9 J cm^{-2}) was found (Zhang et al., 2018).

*Table 3 EC_{50} values (µM) as determined by the (photo)cytotoxicity assay of emodin-1,6-di-O-ß-D-glucopyranoside (**1**), emodin-1-O-ß-D-glucopyranoside (**2**), dermocybin-1-O-ß-D-glucopyranoside (**3**), emodin (**4**), and dermocybin (**5**). The dark cytotoxicity as well as the blue/green light-dependent cytotoxicity (blue light irradiation: λ = 468 ± 27 nm, 9.3 J/cm², green light irradiation: λ = 519 ± 33 nm, 30.0 J/cm²) was evaluated. EC_{50} values in combination with their 95% confidence intervals are given in µM. The photoindex, calculated as the ratio of cells killed in the dark to cells killed under irradiation, is given as well.*

	A549 (BL, 468 nm)	A549 (Dark)	P.I.	AGS (BL, 468 nm)	AGS (Dark)	P.I.	T24 (BL, 468 nm)	T24 (Dark)	P.I.
1	>25.0	>25.0		>25.0	>25.0		>25.0	>25.0	
2*	>25.0	>25.0		>25.0	>25.0		>25.0	>25.0	
3	>25.0	>25.0		>25.0	>25.0		>25.0	>25.0	
4*	2.9 (1.1 / 0.8)	19 (5.3 / 4.1)	7	1.5 (0.9 / 0.6)	>25.0		1.7 (0.6 / 0.4)	>25.0	>15
5	>25.0	>25.0		>25.0	>25.0		>25.0	25	
	A549 (GL, 519 nm)	A549 (Dark)	P.I.	AGS (GL, 519 nm)	AGS (Dark)	P.I.	T24 (GL, 519 nm)	T24 (Dark)	P.I.
3	>25.0	>25.0		>25.0	>25.0		>25.0	>25.0	
5	16.2 (4.1 / 3.3)	>25.0	>1.5	>25.0	>25.0		11.6 (4.4 / 3.2)	24.7 (13 / 9)	2.1

* Adopted from (Hammerle et al., 2021).

6. Conclusion

Here we could show that extracts of the colorful dermocyboid *Cortinarii* are characterized by promising photoantimicrobial activities. While the moderate antimicrobial potential of mushrooms under dark conditions was known already, the exorbitant additional effect of light was studied here in detail for the first time. Under light irradiation, the antimicrobial effect is enhanced, reaching concentrations as low as 0.37 µM and 2.27 µM for the two monomeric anthraquinones emodin (**4**) and dermocybin (**5**). The observed action of **5** under green light irradiation against *S. aureus* is propitious due to its selective character; an *in vitro* cytotoxicity test employing cells of an immortal human stomach cell line (AGS) showed no (photo)cytotoxic effect. Most intriguingly, however, the abundant natural compound emodin (**4**) was highly active against *C. albicans* and *S. aureus* under blue light irradiation (MIC c = 0.1 µg/mL (0.37 µM) and 0.5 µg/mL (1.85 µM)), and active against *E. coli* with a MIC of c = 3 µg/mL (11 µM). While emodin was reported to occur in many plants, insects, lichens, and fungi, this is the first time its promising photoantimicrobial effect has been revealed. A systematic exploration of the many known natural and synthetic anthraquinones might even lead to more promising photoantimicrobial hits.

7. Experimental Part

7.1. Chemicals and Reagents

Solvents were purchased from VWR International (Vienna, Austria) if not stated otherwise. Acetone was distilled prior to use. Solvents for HPLC experiments had pro analysis (p.a.) quality and were obtained from Merck (Merck KGaA, Darmstadt, Germany). Ultrapure water was obtained with the Sartorius arium® 611 UV purification system (Sartorius AG, Göttingen, Germany). Curcumin, dimethylsulfoxid (DMSO), lysogeny broth (LB) agar, and RPMI1640 medium were purchased from Merck KGaA (Darmstadt, Germany). Potato dextrose agar (PDA) and Mueller Hinton Broth (MHB) were purchased from VWR International (Vienna, Austria). The 96-well plates (flat bottom) were bought from Sarstedt (Nümbrecht, Germany).

7.2. Instruments

Desiccation of the fruiting bodies (FB) was done with a dehydrator from Stöckli (A. & J. Stöckli AG, Switzerland) operated at a temperature of 40 °C. The Bosch coffee grinder MKM 6003 (Stuttgart, Germany) was used for grinding. Scales from KERN ALS 220-4 (KERN & SOHN GmbH, Balingen-Frommern, Germany) and Sartorius Cubis®-series (Sartorius AG, Göttingen, Germany) were employed. The ultrasonic bath Sonorex RK 106 (BANDELIN electronic GmbH & Co. KG, Berlin, Germany) was utilized, as well as the Vortex-Genie 2 mixer (Scientific Industries, Inc., Bohemia, New York). For centrifugation, an Eppendorf 5804R centrifuge with a F-45-30-11 - 30 place fixed angle rotor (Hamburg, Germany) was used.

Pipetting was done with pipettes and tips from Eppendorf AG (Hamburg, Germany) and STARLAB International GmbH (Hamburg, Germany). Reagent reservoirs were obtained from Thermo Fischer Scientific (Waltham, Massachusetts, USA).

HPLC measurements were carried out with the modular system Agilent Technologies 1260 Infinity II (Agilent Technologies, Inc., Santa Clara, USA) with a quaternary pump, vial sampler, column thermostat, diode-array detector, and mass spectrometer. Moreover, the HPLC-system Agilent Technologies 1200 Series with a binary pump, autosampler, column thermostat, and diode-array

detector was used. For all HPLC measurements, a Synergi 4 µ MAX-RP 80Å 150 x 4.60 mm column was used. HPLC-DAD-ESI-MS analysis was carried out with the modular system Agilent Technologies 1260 Infinity II equipped with a quaternary pump, vial sampler, column thermostat, diode-array detector, and an ion trap mass spectrometer (amaZon, Bruker, Bremen, Germany). The U-2001 spectrophotometer for adjusting the McFarland standard was from Hitachi (Chiyoda, Japan).

For measurement of the 96-well plates, a Tecan Sunrise Remote Plate Reader (Tecan, Männedorf, Switzerland) was used. The adjustment of pH-values was carried out with the pH-meter Mettler Toledo SevenMulti (Mettler-Toledo GmbH, Vienna, Austria).

Homogenous irradiation of the 96-well plates was achieved by utilizing either the power adaptor Agilent E3611A DC Power Supply (Agilent Technologies, Inc., Santa Clara, United States) in combination with a LED-panel (λ = 468 ± 27 nm (E_m = 20.6 mW cm^{-2}) or λ = 519 ± 33 nm (E_m = 22.3 mW cm^{-2}) (University Leiden, published in Hopkins et al. (Hopkins et al., 2016), characterized in (Siewert et al., 2019)) or the SciLED setup (λ = 428 ± 15 nm (E_m = 13.0 mW cm^{-2}), 478 ± 27 nm (E_m = 8.7 mW cm^{-2}) or λ = 523 ± 33 nm (E_m = 6.0 mW cm^{-2}) published by Fiala and Schöbel et al (Fiala et al., 2021)).

7.3. Mycochemical Part

7.3.1. Fungal Biomaterial and Sample Preparation

The fruiting bodies of *C. cinnabarinus, C. holoxanthus, C. rubrophyllus*, and *C. sanguineus* were collected in Tyrol (Austria) and Abruzzo (Italy). Table S1 contains detailed information and GenBank numbers. A reliable taxonomic classification was achieved by combining macroscopic and microscopic techniques as well as rDNA ITS sequence analysis. After collection and identification, the fresh fruiting bodies were immediately frozen and stored in a freezer at -18 °C or –in the case of *C. cinnabarinus*– dried in a dehydrator at T = 45 °C. Before extraction, the fruiting bodies were freeze-dried, finely ground with mortar and pestle, and stored in paper bags.

7.3.2. Preparation of Fungal Extracts

The fungal biomaterial (Table S1) was dried in a desiccator (T ~ 40 °C) right after collection and stored at room temperature until further use (T = 23.0 °C, humidity = 20 ± 10%). The biomaterials were milled and sieved utilizing a mesh with the size of 400 µm. The extraction process was performed under light exclusion at room temperature. The powdered materials (m = 2.00 g) were extracted with acidified acetone (V = 20 mL, 0.1% v/v 2N HCl) in an ultrasonic bath (t = 10 min). After centrifugation (t = 10 min, T = 4 °C, RCF = 21000 g), acetone was decanted and filtered through cotton wool. The procedure was repeated twice with less acidified acetone (V = 5 mL). The combined supernatants were evaporated and stored in brown glass vials at room temperature (see Table 1 for yields).

7.3.3. Targeted Isolation of *C. sanguineus*

After drying and milling of the *C. sanguineus* fruiting bodies, the biomaterial (m = 34.8 g) was extracted successively with petroleum ether (V = 500 mL, n = 4), dichloromethane (V = 500 mL, n = 6), and methanol (V = 500 mL, n = 10), and water (V = 500 mL, n = 1) utilizing ultrasonication (5 min per extraction step) at room temperature (T = 22.5 °C). Following each extraction step, the extracts were filtered, and the respective filtrates were combined. After solvent evaporation, the extracts were subjected to freeze-drying for removal of any residual solvent. The extraction process yielded η = 577.6 mg (1.7% w/w) of petroleum ether extract, η = 979.6 mg (2.8% w/w) of dichloromethane extract, η = 12665.8 mg (36.4% w/w) of methanol extract, and η = 2913.0 mg (8.4% w/w) of water extract.

Isolation of emodin-1,6-di-*O*-β-D-glucopyranoside (**1**)

An aliquot of the *C. sanguineus* methanol extract (m = 3.27 g) was dissolved in ultrapure water (V = 350 mL), transferred into a separatory funnel, and extracted successively with diethyl ether (Et_2O, V = 400 mL, n = 7), ethyl acetate (EtOAc, V = 300 mL, n = 8), and water-saturated n-butanol (BuOH, V = 200 mL, n = 4) by liquid-liquid extraction. The respective fractions and the residual aqueous phase (H_2O) were dried by vacuum rotary evaporation at 40 °C. Any solvent residues were removed by freeze-drying. The yields of the fractions were as follows: m_{Et2O} = 198.5 mg (6.1% w/w), m_{EtOAc} = 175.8 mg (5.4% w/w), m_{BuOH} = 461.3 mg (14.1% w/w), and m_{H2O} = 2206.0 mg (67.5% w/w). Subsequently, an aliquot of the n-butanol fraction (m = 300.2 mg) was dissolved in ultrapure water (V = 200 mL) and subjected again to a successive liquid-liquid extraction with dichloromethane (BuL1, V = 200 mL, n = 3) and ethyl acetate (BuL2, V = 200 mL, n = 9). Thereafter, the aqueous phase was acidified with glacial acetic acid until the color changed from red to orange and extracted with ethyl acetate (BuL3, V = 200 mL, n = 6). The fractions were dried as described above and the yields determined: m_{BuL1} = 5.8 mg (1.9% w/w), m_{BuL2} = 42.5 mg (14.2% w/w), and m_{BuL3} = 90.7 mg (30.2% w/w).

The residual aqueous phase was submitted to RP-18 solid-phase extraction (RP-18 SPE, stationary phase: LiChroprep® RP-18 (0.040-0.063 mm), Ø = 15 mm, l = 25 mm). After activation of the column with methanol, it was equilibrated with water, and loaded with the aqueous phase. The loaded column (trapped metabolites were visible as a yellow band) was washed with water (V = 20 mL) and then elution was performed with methanol (V ~ 10 mL). The fraction obtained (BuL4) was dried under air flow and yielded a mass of 27.1 mg (7.0% w/w). BuL4 (m = 14.3 mg) was purified by preparative thin-layer chromatography (TLC / stationary phase: pre-coated TLC sheets, 10 x 20 cm, silica gel 60 F254 0.20 mm layer) with toluene/acetone/formic acid/acetic acid (35:40:12.5:12.5) as mobile phase. For this purpose, BuL4 was dissolved in methanol (V ~ 2 mL) and loaded onto seven TLC plates. After separate development (separation distance ~ 8 cm), the yellow band with a Rf-value of 0.2 was removed from each plate, suspended via sonication in water, and purified via RP-18 SPE as described above. Elution of **1** (4.2 mg) was done with acetonitrile.

Emodin-1,6-di-*O*-β-D-glucopyranoside (**1**) was obtained as a yellow solid (η = 4.2 mg, 0.012% w/w). M.p.: no clear m.p. observed (decomposition > 250 °C); $[\alpha]_D^{25}$= -56 (c = 0.10 mg/mL, MeOH); R_f = 0.20 (stationary phase: SiO_2, mobile phase: toluene/acetone/formic acid/acetic acid = 35:40:12.5:12.5); ^{1}H NMR (600 MHz, D_2O, 25 °C) δ = 7.19 (s, 1H, $C_{ar}H$-2), 7.13 (s, 1H, $C_{ar}H$-4), 6.84 (d, *J* = 2.4 Hz, 1H, $C_{ar}H$-5), 6.62 (d, *J* = 2.4 Hz, 1H, $C_{ar}H$-7), 5.14 (d, *J* = 7.6 Hz, 1H, C*H*-1´´), 4.99 (d, *J* = 6.8 Hz, 1H, C*H*-1´), 4.12-4.04 (m, 2H, CH_a-6' + CH_a-6''), 3.97 – 3.88 (m, 2H, CH_b-6' + CH_b-6''), 3.82 – 3.62 (m, 8H, glycosidic H), 2.31 (s, 3H, CH_3-3) ppm; IR (ART): $\tilde{\nu}$ = 3344 (w), 2924 (w), 1629 (w), 1262 (w), 1068 (w) cm^{-1}; MS (ESI, negative mode 4.5 kV) m/z (%) 629.0 (100), 656.0 (85), 431.0 (86), 593.0 (66) $[M-H]^-$; UV-Vis (MeOH): λ_{max} (ε) = 221 (4398), 264 (3551), 414 nm (1328 $mol^{-1}\,dm^3\,cm^{-1}$).

Isolation of emodin-1-*O*-β-D-glucopyranoside (**2**) and dermocybin-1-*O*-β-D-glucopyranoside (**3**)

An aliquot of the methanol extract (m = 1475.9 mg) was dissolved in ultrapure water (V = 150 mL), transferred into a separatory funnel, and extracted successively with diethyl ether (V = 100 mL, n = 8) and ethyl acetate (V = 150 mL, n = 5). The ethyl acetate extracts were combined, dried using vacuum rotary evaporation at 40 °C, and yielded 94.6 mg (6.4% w/w) of fraction called M1. The aqueous phase was then acidified with 20 mL of glacial acetic acid. The acidified phase was extracted once with 100 mL of ethyl acetate, which was set aside. Subsequently, extraction was carried out with ethyl acetate (V = 100 mL, n = 4). The extracts were combined and evaporated to dryness to finally obtain 430.2 mg of fraction M2. M1 (m = 73.2 mg) was further purified via repeated (n = 2) recrystallization from 60% ethanol. Briefly, the aliquot was suspended, heated in a water bath (T = 100 °C) until fully dissolved, and stored in the refrigerator (T = 8 °C) for several hours. The crystallized compound was then

centrifuged, washed with water, and dried under air flow. In this way, 4.7 mg of **2** were obtained. Purification of M2 by recrystallization from 60% ethanol as described above gave 7.7 mg of **3**.

Emodin-1-*O*-β-D-glucopyranoside (**2**) [CAS: 38840-23-2] was isolated as an orange solid (η = 4.7 mg, 0.014% w/w) Identification was achieved via comparison of compound specific properties with reference data (Hammerle et al., 2021). M.p.: 220-228 °C (239-241 °C (Okabe et al., 1973), 210-211 °C (Steglich and Lösel, 1972)); R_f = 0.65 (stationary phase: SiO_2, mobile phase: toluene/acetone/formic acid/acetic acid = 35:40:12.5:12.5); ^{1}H NMR (600 MHz, CD_3OD, 25 °C) δ = 8.51 (s, 1H, $C_{ar}OH$-6), 7.82 (s, 1H, $C_{ar}H$-4), 7.63 (s, 1H, $C_{ar}H$-2), 7.14 (s, 1H, $C_{ar}H$-5), 6.55 (s, 1H, $C_{ar}H$-7), 5.02 (d, *J* = 7.6 Hz, 1H, C*H*-1´), 3.97 (dd, *J* = 12.1, 2.3 Hz, 1H, CH_a-6´), 3.74 (dd, *J* = 12.1, 6.3 Hz, 1H, CH_b-6´), 3.70 – 3.64 (dd, *J* = 9.3, 7.6 Hz, 1H, C*H*-2´), 3.58 – 3.52 (m, 2H, C*H*-3´ & C*H*-5´), 3.46 – 3.42 (dd, *J* = 9.3, 9.3 Hz, 1H, C*H*-4´), 2.50 (s, 3H, CH_3-3) ppm; IR (ART) = $\tilde{\nu}$ = 3215 (w), 2921 (w), 1619 (w), 1594 (w), 1254 (w), 1176 (w), 1057 (w), 1023 (m), 882 (m), 719 (w), 521 (w), 420 (w) cm^{-1}; MS (ESI, negative mode 4.5 kV) m/z (%) 431.7 (100) [M-H]$^-$; UV-Vis (MeOH): λ_{max} (ε) = 212 (25970), 252 (19466), 287 (17096), 428 nm (6239 mol^{-1} dm^3 cm^{-1}).

Dermocybin-1-*O*-β-D-glucopyranoside (**3**) was obtained as a red solid (η = 7.7 mg, 0.022% w/w) with minor impurities of (**2**). M.p.: 232-234 °C (228-230 °C (Steglich and Lösel, 1972)); R_f = 0.55 (stationary phase: SiO_2, mobile phase: toluene/acetone/formic acid/acetic acid = 35:40:12.5:12.5); $[\alpha]_D^{20}$= -88 (c = 0.14 mg/mL, MeOH); ^{1}H NMR (600 MHz, CD_3OD, 25 °C) δ 7.90 (s, 1H, $C_{ar}H$-4), 7.59 (s, 1H, $C_{ar}H$-2), 5.06 (d, *J* = 7.7 Hz, 1H, C*H*-1´), 4.02 (s, 3H, OCH_3-6), 3.99 (dd, J = 12.1, 2.3 Hz, 1H, CH_a-6´), 3.77 (dd, J = 12.1, 6.2 Hz, 1H, CH_b-6´), 3.72 – 3.65 (m, 1H, C*H*-2´), 3.61 – 3.54 (m, 2H, C*H*-3´ & C*H*-5´), 3.49 – 3.44 (m, 1H, C*H*-4´), 2.53 (s, 3H, CH_3-3) ppm; IR (ART) = $\tilde{\nu}$ = 3413 (w), 2917 (w), 1588 (w), 1471 (w), 1408 (w), 1299 (w), 1035 (w), 634 (w), 550 (w), cm^{-1}; MS (ESI, negative mode 4.5 kV) m/z (%) 477.1 (100) [M-H]$^-$; UV-Vis (MeOH): λ_{max} (ε) = 215 (33720), 264 (29257), 301 (shoulder / 14554), 485 (10781), 525 nm (shoulder / 6464 mol^{-1} dm^3 cm^{-1}).

Isolation of emodin (4)

An aliquot (m = 500.1 mg) of the dichloromethane extract was subjected to acetylated polyamide column chromatography (Ø = 2.5 cm, l = 45 cm). First, isocratic elution was performed with petroleum ether (V = 200 mL), followed by elution with petroleum ether/toluene (8:2 v/v, V = 100 mL, D1.), toluene (V = 700 mL), toluene/chloroform (9:1 v/v, V = 300 mL), toluene/chloroform (7:3 v/v, V = 200 mL), and lastly chloroform ($V_{CHCl3|1}$ = 450 mL, $V_{CHCl3|2}$ = 300 mL). Concentration of the second chloroform eluate (i.e., $V_{CHCl3|2}$: approximately 50% of the starting volume left) via rotary evaporation *in vacuo* resulted in the precipitation of orange crystals. The precipitate was filtered off and dried to obtain 79.7 mg of **4**.

Emodin (**4**) [CAS: 518-82-1] was isolated as an orange solid (η = 79.7 mg, 0.23% w/w). M.p.: 260 °C (253-254 °C (Kögl and Postowsky, 1925)); R_f = 0.65 (stationary phase: SiO_2; mobile phase: toluene/ethyl acetate/formic acid/acetic acid (70:20:5:5); ^{1}H NMR (600 MHz, DMSO-d6, 25 °C) δ = 12.09 (s, 1H, C_{ar}-O*H*-8), 12.02 (s, 1H, C_{ar}-O*H*-1), 11.34 (brs, 1H, C_{ar}-O*H*-6), 7.51 (d, *J* = 1.6 Hz, 1H, $C_{ar}H$-4), 7.18 (d, *J* = 1.8 Hz, 1H, $C_{ar}H$-2), 7.13 (d, *J* = 2.4 Hz, 1H, $C_{ar}H$-5), 6.60 (d, *J* = 2.4 Hz, 1H, $C_{ar}H$-7), 2.47 ppm (s, 3H, CH_3-3) MS (ESI, negative mode 4.5 kV) m/z (%) 269.0 (100) [M-H]$^-$; UV-Vis (MeOH): λ_{max} (ε) = 226 (16806), 287 (17167), 436 nm (10724 mol^{-1} dm^3 cm^{-1}).

Isolation of dermocybin (5)

Aliquots of the water extract (m = 1636.6 mg) and the water fraction (m = 1066.8 mg) were combined, dissolved in ultrapure water, transferred into a separatory funnel, and extracted successively with diethyl ether (W1, V = 250 mL, n = 3) and ethyl acetate (W2, V = 300 mL, n = 4). Then, the aqueous phase was acidified with glacial acetic acid (V = 30 mL). The acidified phase was extracted five times with ethyl acetate (V = 300 mL), the first two extracts being combined to fraction W3 and the last three

to fraction W4. Solvents were removed using vacuum rotary evaporation at 40 °C and freeze-drying. The resulting fractions gave following yields: m_{W1} = 54.4 mg (2.0% w/w), m_{W2} = 10.1 mg (0.4% w/w), m_{W3} = 7.5 mg (0.3% w/w), and m_{W4} = 181.8 mg (6.7% w/w). Fraction W1 (m = 21.0 mg) was dissolved in a mixture containing equal volumes of diethyl ether and dichloromethane (V = 50 mL), transferred into a separatory funnel, and extracted with saturated Na_2HPO_4 solution (V = 50 mL, n = 3). The resulting fractions were combined, acidified with concentrated hydrochloric acid (q.s. for color change from purple to yellow), and extracted twice with 50 mL of diethyl ether/dichloromethane (1:1 v/v). The combined fractions were then evaporated to dryness and yielded 9.3 mg of crude dermocybin (W1.1). W.1.1 was further purified by suspending the dried fraction in a small volume of acetone (q.s. to 50% dissolution) and adding saturated Na_2HPO_4 solution until completely dissolved. Then the solution was diluted with six times the amount of ultrapure water and extracted with diethyl ether (V = 100 mL, n = 2). Thereafter, the aqueous phase was acidified with concentrated hydrochloric acid (q.s. until color change from red to yellow) and extracted once with diethyl ether (W1.2, V = 100 mL). After drying as described above, fraction W1.2 yielded 6.3 mg of **5**.

Dermocybin (**5**) [CAS: 7229-69-8] was obtained as a red solid (η = 6.3 mg, 0.018% w/w). M.p.: 220-222 °C (228-229 °C (Kögl and Postowsky, 1925)); R_f = 0.60 (stationary phase: SiO_2; mobile phase: toluene/ethyl acetate/formic acid/acetic acid (70:20:5:5); ^{1}H NMR (600 MHz, $(CD_3)_2CO$, 25 °C) δ = 13.88 (s, 1H, C_{ar}-O*H*-5), 12.61 (d, *J* = 12.6 Hz, 1H, C_{ar}-O*H*-8), 12.06 (d, *J* = 15.3 Hz, 1H, C_{ar}-O*H*-1), 9.64 (s, 1H, C_{ar}-O*H*-7), 7.67 (s, 1H, C_{ar}*H*-4), 7.15 (s, 1H, C_{ar}*H*-2), 4.05 (s, 3H, OCH_3-6), 2.50 ppm (s, 3H, CH_3-3); MS (ESI, negative mode 4.5 kV) m/z (%) 315.0 (100) $[M-H]^-$; UV-Vis (MeOH): $\boldsymbol{\lambda_{max}}$ (ε) = 219 (31518), 262 (28581), 277 (shoulder / 23518), 301 (12665), 484 (14567), 519 nm (shoulder / 10685 $mol^{-1}\,dm^3\,cm^{-1}$).

7.3.4. Singlet-Oxygen Detection via the DMA-Assay

The previously described 9,10-dimethyl anthracene (DMA) assay was employed (Siewert et al., 2019) to analyze the ability of the six fungal extracts to generate singlet oxygen after irradiation. In brief, four stock solutions were prepared: a DMA solution in ethanol (c = 0.35 mM), a DMA-solution (c = 0.35 mM) containing L-ascorbic acid (c = 5 mM) in ethanol, L-ascorbic acid (c = 5 mM) in ethanol, and pure ethanol (96%). The fungal extracts were dissolved in DMSO (c = 1 mg/mL), mixed with the stock solutions, transferred into a 96-well plate yielding a fungal extract concentration of c = 0.05 mg/mL per well. DMSO (V = 10 µL, 5%) was used as negative control, berberine (c = 0.15 mM) and RB (c = 5 µM) were used as positive controls. Thereafter, the multiwell plates were irradiated by four cycles of blue light (λ = 468 nm, 1.24 J $cm^{-2}\,min^{-1}$, berberine = positive control) or of green light irradiation (λ = 519 nm, 0.92 J $cm^{-2}\,min^{-1}$, rose bengal = positive control). All measurements were done as technical duplicates. The results of the DMA-assay were presented as the mean ± standard error.

7.3.5. Determination of the singlet oxygen photoyield via NIR measurements

The steady-state singlet oxygen emission measurements were performed on a previously reported custom-built setup utilising a slightly modified experimental procedure (Zhou et al., 2019; Partanen et al., 2020; Ossola et al., 2021). Perinaphthenone was used as a reference with reported ϕ_Δ ($^1O_2$) = 0.98 ± 0.07 in air-saturated ACN and ϕ_Δ ($^1O_2$) = 0.97 ± 0.04 in air-saturated CD_3OD (Oliveros et al., 1991; Schmidt et al., 1994). $Ru(bpy)_3Cl_2$ was used as validation compound with reported ϕ_Δ ($^1O_2$) = 0.57 ± 0.06 in air-saturated ACN and ϕ_Δ (1O2) = 0.73 ± 0.12 in air-saturated CD_3OD (Garcìa-Fresnadillo et al., 1996; Abdel-Shafi et al., 2000). All the compounds were dissolved in ACN or CD_3OD (V = 3 mL) and transferred into a macro fluorescence cuvette from Firefly (lightpaths: 1 cm x 1 cm). The irradiation of samples was done at 298 K using 450 nm LRD-0450 Laserglow fiber-coupled laser set to 80 mW at the cuvette with help of PM100USB Thorlabs power meter. The UV-Vis and NIR spectra were recorded at 298 K with Agilent Cary 60 UV-Vis and Avantes NIR256-1.7TEC spectrometers respectively. The NIR emission spectrums were acquired within 20 s. All the spectral data was processed with OriginPro 9.1 and Microsoft Office Excel 2016.

7.3.6. GC-MS Analyses of the Sugar Residue

Spectral data of **3** pointed towards β-glucose-substituted **5**. To determine the absolute configuration of the glucose residue, a GC-MS analysis was carried out. Crude methanolic extract of *C. sanguineus* (m = 15.9 mg), a n-butanol fraction (m = 10.0 mg), and an ethyl acetate fraction (fraction M2, m = 3.8 mg) were separately solved in aqueous trifluoroacetic acid (TFA, c = 3 mol/L, V = 1 mL) and heated at T = 90 °C for 60 minutes. After cooling and addition of water (V = 2 mL), the reaction mixture was extracted three times with ethyl acetate (V = 2 mL). The aqueous phase was dried under an air stream at room temperature and kept in a desiccator. D-Glucose (m = 1.0 mg, n = 5.5 µmol), L-glucose (m = 1.0 mg, n = 5.5 µmol), and the dried hydrolysate were derivatized with L-cysteine methyl ester hydrochloride (1.5 mg (8.7 µmol) in 200 µL pyridine, T = 60 °C, t = 60 min), subsequently silylated with *N,O*-bis(trimethylsilyl)trifluoroacetamide and chlorotrimethylsilane (BSTFA:TMCS = 99:1, 200 µL, T = 60 °C, t = 60 min), and analyzed using GC-MS. GC-MS analysis was carried out on an Agilent 5975C Series GC/MSD System equipped with an Agilent 7693 autosampler, and a Triple Axis-Detector (MS). An Agilent 19091S-433: 1813.75629 HP-5MS 5% Phenyl Methyl Silox (325 °C: 30 m x 250 µm x 0.25 µm) column was used as stationary phase and helium served as carrier gas. The oven temperature was first set to T = 170 °C. After the temperature was kept constant at T = 170 °C for five minutes, the oven was brought up to 270 °C with a heating rate of 3 °C/min. The oven was then heated to 320 °C at 20 °C/min and kept at this temperature for additional five minutes. The total run time, injection volume, split ratio, and flow rate were set to t = 45.8 min, V = 1 µL, 50:1, and Q = 0.75 mL/min, respectively. The results of the GC-MS analysis are depicted in Figure S18.

7.4. Microbiological Testing

7.4.1. Strains and Cultivation

If not stated differently, all experiments were done as described previously (Fiala et al., 2021). In brief, the strains used in this study were *Candida albicans* (501670), *Escherichia coli* (DSM1103), and *Staphylococcus aureus* (DSM1104). The bacterial cultures were stored in darkness at T = 4°C on lysogeny broth (LB) agar. *C. albicans* was cultivated on potato dextrose agar (PDA) under the same conditions. For the PACT experiments, the stored cultures were reactivated, and an overnight culture was incubated (T = 37°C, t = 15 - 18 h, dark conditions). Turbidity was adjusted to a McFarland standard of 0.5 to prepare the standard suspensions. For yeast suspensions, turbidity was measured at λ = 530 nm. For bacteria suspensions, turbidity was measured at λ = 600 nm. Liquid media used for PACT experiments were Müller-Hilton broth for bacteria and RPMI-1640 (double strength) for yeast.

7.4.2. PhotoMIC Assay

The photoantimicrobial experiments were performed as previously published. In short, two identical 96-well plates were prepared for the dark and light treatment. On each plate, the extracts were tested (i.e., c = 5 µg/mL, 25 µg/mL, and 50 µg/mL), fraction-blanks and medium-blanks measured, and the untreated population recorded as growth control. If needed, the concentrations were adjusted to identify the break point. Curcumin, as an established photosensitizer, was utilized as a positive control (Fiala et al., 2021). Bacterial cultures were adjusted via photometry to 0.5 McFarland standard in water and diluted in Müller-Hilton broth (1:50). Yeast suspensions adjusted to a 0.5 McFarland standard were diluted with RPMI-1640 (double strength, 1:10). Within thirty minutes after diluting the suspensions, the plates were inoculated (V = 50 µL) to reach 2-8 x 10^5 CFU/mL for bacteria (Franklin R. Cockerill et al., 2012) and 0.5-2.5 x 10^5 CFU/mL for yeast (Rodriguez-Tudela et al., 2008). After ten or sixty minutes of preincubation time in the dark, one plate was irradiated with a light dose of H = 30 J/cm^2. The other plate was kept in the darkness at room temperature. Viability controls were drawn and plated on LB agar/PDA. The 96-well plates and LB agar/PDA plates were incubated at T = 37 °C in the dark. After 20 - 24 hours, turbidity measurements were done after shaking for fifteen seconds, followed by taking samples of wells that showed inhibition (>20%) of population growth control.

Assessment of the PACT experiment was done by correlating the treated well to the uninhibited growth control. Turbidity of fraction-blank and medium-blank was subtracted from corresponding wells to eliminate deviation caused by darkening or bleaching of media and extracts. Each concentration of fungal extracts, the positive control, and the growth control were measured at least in triplicates.

7.5. (Photo)cytotoxicity Assay

Cells of the adherent cancer cell lines A549 (non-small cell lung cancer, ATCC, Sigma-Aldrich), AGS (stomach cancer, CLS, Eppelheim), and T24 (urinary bladder carcinoma, CLS, Eppelheim) were cultivated in 75 cm^2 Nunc EasYFlasks (product number: 51985042, 75 cm^2) with Gibco™ MEM™-medium (product number: 42360081) supplemented with fetal calf serum (FCS, 10% v/v) and penicillin/streptomycin (P/S, 1% v/v). Cells were trypsinized every other day (confluency ~ 80%) and used for 8-12 weeks. Freezing and thawing of cell cultures was done according to standard procedures. The (photo)cytotoxicity assay was performed as published elsewhere (Hopkins et al., 2016; Siewert et al., 2019).

Briefly, cells (AGS: 2500 cells/well, T24: 1500 cells/well, A549: 2000 cells/well) were seeded in 96-well plates in Gibco™ Opti-MEM™ (OMEM, product number: 11058021) containing FCS (2.4% v/v) and P/S (1% v/v) at 37 °C in 5% CO_2 atmosphere. The extracts/fractions were dissolved in DMSO ($c_{stock\ solution}$ = 10 mg/mL) and further diluted with OMEM. The cells were treated 24 hours after seeding with six different working solutions per extract/fraction. The final concentrations tested were 55.0, 27.5, 11.0, 5.5, 2.8, and 0.6 µg/mL for the extracts and 50.0, 25.0, 10.0, 5.0, 2.5, and 0.5 µg/mL for the fractions. Pure compounds were dissolved in DMSO (c = 5.0 mM) and diluted with OMEM to finally obtain test solutions with the following concentrations: 25.0, 12.5, 5.0, 2.5, 1.3, and 0.3 µM. After incubating the cells for additional 24 hours, the medium was aspirated and replaced by fresh OMEM (+ 2.4% v/v FCS, + 1% P/S). Of two identically treated plates one was irradiated for 7 minutes 30 seconds with blue light (λ = 468 nm ± 27 nm, H = 9.3 J cm^{-2}) / 22 minutes 23 seconds with green light (λ = 519 nm ± 33 nm, H = 30.0 J cm^{-2}) and the other one kept in the dark (light-independent/dark cytotoxicity). After the irradiation step, the plates were kept at 37 °C in 5% CO_2 atmosphere for another 48 hours (total experiment time = 96 hours). Then, the cells were fixed by careful addition of cold trichloroacetic acid (10% w/v in water, V = 100 µL/well) and stored in a refrigerator at 8 °C for at least 24 hours. The fixed

cell-monolayers were washed with slow running deionized tap-water and stained with sulforhodamin B (SRB) (acid red 52, 0.4% w/v SRB in 1% v/v acetic acid, V = 100 µL/well) for 30 minutes. Thereafter, the plates were washed again (n = 5, 1% v/v acetic acid) and dried at room temperature. The dried dye was then redissolved in tris(hydroxymethyl)aminomethane-solution (TRIS, 10 mM in water, V = 100 µL/well) and incubated for at least 20 minutes. Absorbance was measured at λ = 540 nm with a plate reader. EC_{50} values including their confidence intervals (95%) were calculated with GraphPad Prism 5 employing the relative Hill-Slope equation ("log(inhibitor) vs. normalized response -- Variable slope"). As negative control served the illuminated, non-treated cells as well as the non-illuminated, non-treated cells. The photoindex (P.I.), which expresses the ratio of cells killed in the absence of light to cells killed after irradiation, was calculated as $EC_{50|dark}$ divided by $E_{C50|irradiated}$. Treated cells were microscopically investigated (Figure S18-20).

8. Funding

The Tyrolian Science fund is acknowledged for the funding of the irradiation setup and the collection.

The Austrian Science Fund (FWF, P31915) is kindly acknowledged for its financial support.

9. Author Contribution

L.H. collected the fungal species and identified them with U.P.; A.H. and F.H. prepared the fungal extracts, characterized them together with B.S., and isolated the pure compounds; J.F. performed and analyzed the photoantimicrobial testing together with B.S.; A.H. and F.H. conducted the cell biological testing; Y.H. performed and analyzed the photochemical investigations under the supervision of S.B.; B.S. designed the research, supervised it, and wrote the first draft. All authors corrected and approved the final manuscript.

10. Acknowledgment

H. Stuppner and C. Schinagl are thanked for their valuable input and the fruitful discussions. N. Engels´ proof-reading is highly acknowledged.

11. References

Abdel-Shafi, A.A., Beer, P.D., Mortimer, R.J., and Wilkinson, F. (2000). Photosensitized Generation of Singlet Oxygen from Vinyl Linked Benzo-Crown-Ether−Bipyridyl Ruthenium(II) Complexes. *The Journal of Physical Chemistry A* 104(2), 192-202. doi: 10.1021/jp991876z.

Aroso, R.T., Calvete, M.J.F., Pucelik, B., Dubin, G., Arnaut, L.G., Pereira, M.M., et al. (2019). Photoinactivation of microorganisms with sub-micromolar concentrations of imidazolium metallophthalocyanine salts. *European Journal of Medicinal Chemistry* 184, 111740. doi: https://doi.org/10.1016/j.ejmech.2019.111740.

Bara, R., Zerfass, I., Aly, A.H., Goldbach-Gecke, H., Raghavan, V., Sass, P., et al. (2013). Atropisomeric Dihydroanthracenones as Inhibitors of Multiresistant Staphylococcus aureus. *Journal of Medicinal Chemistry* 56(8), 3257-3272. doi: 10.1021/jm301816a.

Beattie, K.D., Rouf, R., Gander, L., May, T.W., Ratkowsky, D., Donner, C.D., et al. (2010). Antibacterial metabolites from Australian macrofungi from the genus Cortinarius. *Phytochemistry* 71(8), 948-955. doi: https://doi.org/10.1016/j.phytochem.2010.03.016.

Bresolí-Obach, R., Gispert, I., Peña, D.G., Boga, S., Gulias, Ó., Agut, M., et al. (2018). Triphenylphosphonium cation: A valuable functional group for antimicrobial photodynamic therapy. *Journal of Biophotonics* 11(10), e201800054. doi: https://doi.org/10.1002/jbio.201800054.

Fiala, J., Schöbel, H., Vrabl, P., Dietrich, D., Hammerle, F., Artmann, D.J., et al. (2021). A New High-Throughput-Screening-Assay for Photoantimicrobials Based on EUCAST Revealed Unknown Photoantimicrobials in Cortinariaceae. *Frontiers in Microbiology* 12(2124). doi: 10.3389/fmicb.2021.703544.

Fisher, J.F., and Mobashery, S. (2016). Endless resistance. Endless antibiotics? *MedChemComm* 7(1), 37-49. doi: 10.1039/C5MD00394F.

Franklin R. Cockerill, Matthew A. Wikler, Jeff Alder, N., M., Dudley, G.M.E., Mary Jane Ferraro, et al. (2012). CLSI. Methods for Dilution Antimicrobial Susceptibility Tests for Bacteria That Grow Aerobically; Approved Standard—Ninth Edition. *CLSI document* M07-A9, 1-63.

Galstyan, A. (2021). Turning Photons into Drugs: Phthalocyanine-Based Photosensitizers as Efficient Photoantimicrobials. *Chemistry* 27(6), 1903-1920. doi: 10.1002/chem.202002703.
Galstyan, A., and Dobrindt, U. (2018). Breaching the wall: morphological control of efficacy of phthalocyanine-based photoantimicrobials. *J Mater Chem B* 6(28), 4630-4637. doi: 10.1039/c8tb01357h.
Garcìa-Fresnadillo, D., Georgiadou, Y., Orellana, G., Braun, A.M., and Oliveros, E. (1996). Singlet-Oxygen (1Δg) Production by Ruthenium(II) complexes containing polyazaheterocyclic ligands in methanol and in water. *Helvetica Chimica Acta* 79(4), 1222-1238. doi: https://doi.org/10.1002/hlca.19960790428.
Gill, M., and Steglich, W. (1987). *Fortschritte der Chemie organischer Naturstoffe / Progress in the Chemistry of Organic Natural Products.*
Gollnick, K., Held, S., Mártire, D.O., and Braslavsky, S.E. (1992). Hydroxyanthraquinones as sensitizers of singlet oxygen reactions: quantum yields of triplet formation and singlet oxygen generation in acetonitrile. *Journal of Photochemistry and Photobiology A: Chemistry* 69(2), 155-165. doi: https://doi.org/10.1016/1010-6030(92)85273-W.
Hammerle, F., Bingger, I., Pannwitz, A., Magnutzki, A., Gstir, R., Rutz, A., et al. (2022a). Targeted isolation of photoactive pigments from mushrooms yielded a highly potent new photosensitizer: 7,7′-biphyscion. *Scientific Reports* 12(1), 1108. doi: 10.1038/s41598-022-04975-9.
Hammerle, F., Steger, L.-M., Zhou, X., Bonnet, S., Huymann, L., Peintner, U., et al. (2022b). Optimized isolation of 7,7′-biphyscion starting from Cortinarius rubrophyllus, a chemically unexplored fungal species rich in photosensitizers. *Photochemical & Photobiological Sciences* 21(2), 221-234. doi: 10.1007/s43630-021-00159-y.
Hammerle, F., Steger, L.-M., Zhou, X., Bonnet, S., Huymann, L., Peintner, U., et al. (2021). Optimized Isolation of 7,7′-Biphyscion Starting from Cortinarius rubrophyllus, a Chemically Unexplored Fungal Species Rich in Photosensitizers. *Photochemical & Photobiological Sciences* revision submitted.
Hopkins, S.L., Siewert, B., Askes, S.H.C., Veldhuizen, P., Zwier, R., Heger, M., et al. (2016). An in vitro cell irradiation protocol for testing photopharmaceuticals and the effect of blue, green, and red light on human cancer cell lines. *Photochemical & Photobiological Sciences* 15(5), 644-653. doi: 10.1039/C5PP00424A.
Klausen, M., Ucuncu, M., and Bradley, M. (2020). Design of Photosensitizing Agents for Targeted Antimicrobial Photodynamic Therapy. *Molecules* 25(22), 5239.
Kögl, F., and Postowsky, J.J. (1925). Untersuchungen über Pilzfarbstoffe. II. Über die Farbstoffe des blutroten Hautkopfes (Dermocybe sanguinea Wulf.). *Justus Liebigs Annalen der Chemie* 444(1), 1-7. doi: https://doi.org/10.1002/jlac.19254440102.
Lan, M., Zhao, S., Liu, W., Lee, C.-S., Zhang, W., and Wang, P. (2019). Photosensitizers for Photodynamic Therapy. *Advanced Healthcare Materials* 8(13), 1900132. doi: https://doi.org/10.1002/adhm.201900132.
Liimatainen, K., Kim, J.T., Pokorny, L., Kirk, P.M., Dentinger, B., and Niskanen, T. (2022). Taming the beast: a revised classification of Cortinariaceae based on genomic data. *Fungal Diversity* 112(1), 89-170. doi: 10.1007/s13225-022-00499-9.
Ma, W., Zhang, M., Cui, Z., Wang, X., Niu, X., Zhu, Y., et al. (2021). Aloe-emodin-mediated antimicrobial photodynamic therapy against dermatophytosis caused by Trichophyton rubrum. *Microbial Biotechnology* 15(2), 499-512. doi: 10.1111/1751-7915.13875.
Maisch, T., Eichner, A., Späth, A., Gollmer, A., König, B., Regensburger, J., et al. (2014). Fast and Effective Photodynamic Inactivation of Multiresistant Bacteria by Cationic Riboflavin Derivatives. *PLOS ONE* 9(12), e111792. doi: 10.1371/journal.pone.0111792.
Mulani, M.S., Kamble, E.E., Kumkar, S.N., Tawre, M.S., and Pardesi, K.R. (2019). Emerging Strategies to Combat ESKAPE Pathogens in the Era of Antimicrobial Resistance: A Review. *Frontiers in Microbiology* 10(539). doi: 10.3389/fmicb.2019.00539.
O'Neill, J. (2016). Tackling drug-resistant infections globally: final report and recommendations.
Okabe, H., Matsuo, K., and Nishioka, I. (1973). Studies on Rhubarb (Rhei Rhizoma). II. Anthraquinone Glycosides. *Chemical & Pharmaceutical Bulletin* 21(6), 1254-1260. doi: 10.1248/cpb.21.1254.
Oliveira, D.M.P.D., Forde, B.M., Kidd, T.J., Harris, P.N.A., Schembri, M.A., Beatson, S.A., et al. (2020). Antimicrobial Resistance in ESKAPE Pathogens. *Clinical Microbiology Reviews* 33(3), e00181-00119. doi: doi:10.1128/CMR.00181-19.
Oliveros, E., Suardi-Murasecco, P., Aminian-Saghafi, T., Braun, A.M., and Hansen, H.-J. (1991). 1H-Phenalen-1-one: Photophysical Properties and Singlet-Oxygen Production. *Helvetica Chimica Acta* 74(1), 79-90. doi: https://doi.org/10.1002/hlca.19910740110.
Ossola, R., Jönsson, O.M., Moor, K., and McNeill, K. (2021). Singlet Oxygen Quantum Yields in Environmental Waters. *Chemical Reviews* 121(7), 4100-4146. doi: 10.1021/acs.chemrev.0c00781.
Pang, X., Li, D., Zhu, J., Cheng, J., and Liu, G. (2020). Beyond Antibiotics: Photo/Sonodynamic Approaches for Bacterial Theranostics. *Nano-Micro Letters* 12(1), 144. doi: 10.1007/s40820-020-00485-3.
Partanen, S.B., Erickson, P.R., Latch, D.E., Moor, K.J., and McNeill, K. (2020). Dissolved Organic Matter Singlet Oxygen Quantum Yields: Evaluation Using Time-Resolved Singlet Oxygen Phosphorescence. *Environmental Science & Technology* 54(6), 3316-3324. doi: 10.1021/acs.est.9b07246.
Ran, B., Wang, Z., Cai, W., Ran, L., Xia, W., Liu, W., et al. (2021). Organic Photo-antimicrobials: Principles, Molecule Design, and Applications. *Journal of the American Chemical Society* 143(43), 17891-17909. doi: 10.1021/jacs.1c08679.
Rice, L.B. (2008). Federal Funding for the Study of Antimicrobial Resistance in Nosocomial Pathogens: No ESKAPE. *The Journal of Infectious Diseases* 197(8), 1079-1081. doi: 10.1086/533452.
Rodriguez-Tudela, J.L., Arendrup, M.C., Barchiesi, F., Bille, J., Chryssanthou, E., Cuenca-Estrella, M., et al. (2008). EUCAST Definitive Document EDef 7.1: method for the determination of broth dilution MICs of antifungal agents for

fermentative yeasts: Subcommittee on Antifungal Susceptibility Testing (AFST) of the ESCMID European Committee for Antimicrobial Susceptibility Testing (EUCAST). *Clinical Microbiology and Infection* 14(4), 398-405. doi: 10.1111/j.1469-0691.2007.01935.x.

Schmidt, R., Tanielian, C., Dunsbach, R., and Wolff, C. (1994). Phenalenone, a universal reference compound for the determination of quantum yields of singlet oxygen O2(1Δg) sensitization. *Journal of Photochemistry and Photobiology A: Chemistry* 79(1), 11-17. doi: https://doi.org/10.1016/1010-6030(93)03746-4.

Siewert, B. (2021). Does the chemistry of fungal pigments demand the existence of photoactivated defense strategies in basidiomycetes? *Photochemical & Photobiological Sciences*. doi: 10.1007/s43630-021-00034-w.

Siewert, B., Curak, G., Hammerle, F., Huymann, L., Fiala, J., and Peintner, U. (2022). The photosensitizer emodin is concentrated in the gills of the fungus Cortinarius rubrophyllus. *Journal of Photochemistry and Photobiology B: Biology* 228. doi: 10.1016/j.jphotobiol.2022.112390.

Siewert, B., Vrabl, P., Hammerle, F., Bingger, I., and Stuppner, H. (2019). A convenient workflow to spot photosensitizers revealed photo-activity in basidiomycetes. *RSC Advances* 9(8), 4545-4552. doi: 10.1039/C8RA10181G.

Sperandio, F.F., Huang, Y.-Y., and Hamblin, R.M. (2013). Antimicrobial Photodynamic Therapy to Kill Gram-negative Bacteria. *Recent Patents on Anti-Infective Drug Discovery* 8(2), 108-120. doi: http://dx.doi.org/10.2174/1574891X113089990012.

Steglich, W., and Lösel, W. (1972). Pilzpigmente, X. Anthrachinon-glucoside aus Dermocybe sanguinea (Wulf. ex Fr.) Wünsche. *Chemische Berichte* 105(9), 2928-2932. doi: https://doi.org/10.1002/cber.19721050916.

Steglich, W., Lösel, W., and Austel, V. (1969). Pilzpigmente, IV. Anthrachinon-Pigmente aus Dermocybe sanguinea (Wulf. ex Fr.) Wünsche und D. semisanguinea (Fr.). *Chemische Berichte* 102(12), 4104-4118. doi: https://doi.org/10.1002/cber.19691021217.

Tacconelli, E., Carrara, E., Savoldi, A., Harbarth, S., Mendelson, M., Monnet, D.L., et al. (2018). Discovery, research, and development of new antibiotics: the WHO priority list of antibiotic-resistant bacteria and tuberculosis. *The Lancet Infectious Diseases* 18(3), 318-327. doi: https://doi.org/10.1016/S1473-3099(17)30753-3.

Wainwright, M. (2018). Synthetic, small-molecule photoantimicrobials - a realistic approach. *Photochemical and Photobiological Sciences* 17(11), 1767-1779. doi: 10.1039/c8pp00145f.

Wainwright, M. (2019). Photoantimicrobials and PACT: what's in an abbreviation? *Photochemical and Photobiological Sciences* 18(1), 12-14. doi: 10.1039/c8pp00390d.

Wainwright, M. (2020). A New Penicillin? *Antibiotics (Basel)* 9(3). doi: 10.3390/antibiotics9030117.

Wainwright, M., Antczak, J., Baca, M., Loughran, C., and Meegan, K. (2015). Phenothiazinium photoantimicrobials with basic side chains. *Journal of Photochemistry and Photobiology B: Biology* 150, 38-43. doi: https://doi.org/10.1016/j.jphotobiol.2014.12.017.

Wainwright, M., Maisch, T., Nonell, S., Plaetzer, K., Almeida, A., Tegos, G.P., et al. (2017). Photoantimicrobials - are we afraid of the light? *The Lancet Infectious Diseases* 17(2), e49-e55. doi: 10.1016/S1473-3099(16)30268-7.

Wegener, M., Hansen, M.J., Driessen, A.J.M., Szymanski, W., and Feringa, B.L. (2017). Photocontrol of Antibacterial Activity: Shifting from UV to Red Light Activation. *Journal of the American Chemical Society* 139(49), 17979-17986. doi: 10.1021/jacs.7b09281.

WHO (2017). *Global priority list of antibiotic resistant bacteria to guide research, discovery, and development of new antibiotics* [Online]. https://www.who.int/medicines/publications/WHO-PPL-Short_Summary_25Feb-ET_NM_WHO.pdf. [Accessed 28.12.2021 2021].

Zhang, J.-n., Zhang, F., Tang, Q.-j., Xu, C.-s., and Meng, X.-h. (2018). Effect of photodynamic inactivation of Escherichia coli by hypericin. *World Journal of Microbiology and Biotechnology* 34(7), 100. doi: 10.1007/s11274-018-2464-1.

Zhou, X.-Q., Busemann, A., Meijer, M.S., Siegler, M.A., and Bonnet, S. (2019). The two isomers of a cyclometallated palladium sensitizer show different photodynamic properties in cancer cells. *Chemical Communications* 55(32), 4695-4698. doi: 10.1039/C8CC10134E.